

## Thermodynamic modeling of the deposition of Si–C–N films from the gas phase during the decomposition of organosilicon compounds

V. A. Shestakov,\* E. N. Ermakova, S. V. Sysoev, V. I. Kosyakov, and M. L. Kosinova

A. V. Nikolaev Institute of Inorganic Chemistry Siberian Branch of the Russian Academy of Sciences,  
3 prosp. Akad. Lavrent'eva, 630090 Novosibirsk, Russian Federation.  
Fax: +7 (383) 330 9490. E-mail: vsh@niic.nsc.ru

Thermodynamic modeling of the process of chemical vapor deposition (CVD) of  $\text{SiC}_x\text{N}_y$  and  $\text{SiC}_x\text{N}_y$  films from the gas phase was carried out using organosilicon compounds ( $\text{EtN}(\text{SiMe}_3)_2$ ,  $\text{PhN}(\text{SiMe}_3)_2$ , and  $\text{PhSiMe}_3$ ) at reactor pressures of 0.01 and 10 Torr in the temperature range of 500–1200 K. It was established that regions of existence of two phase complexes, namely,  $\text{SiC} + \text{Si}_3\text{N}_4 + \text{C}$  and  $\text{SiC} + \text{C}$ , were present on the CVD diagrams calculated for the  $\text{EtN}(\text{SiMe}_3)_2\text{--He}$  and  $\text{PhN}(\text{SiMe}_3)_2\text{--He}$  systems. The CVD diagrams calculated for the  $\text{EtN}(\text{SiMe}_3)_2\text{--NH}_3$ ,  $\text{PhN}(\text{SiMe}_3)_2\text{--NH}_3$ , and  $\text{PhSiMe}_3\text{--NH}_3$  systems have regions of existence of three phase complexes, namely,  $\text{Si}_3\text{N}_4 + \text{C}$ ,  $\text{SiC} + \text{Si}_3\text{N}_4 + \text{C}$ , and  $\text{SiC} + \text{C}$ . The composition of the obtained silicon-containing films was calculated.

**Key words:** thermodynamic modeling, CVD diagram, chemical deposition from the gas phase, organosilicon compounds.

Materials based on the phases of the Si–C–N–H system combine good mechanical (rigidity, wear resistance, low friction coefficient, high adhesion to structural materials), chemical (high thermal and corrosion resistance), and physical properties (low dielectric constant, optical transparency in a wide spectral range, a refractive index and an optical band gap controllable in a large range of values, high hydrophobicity), leading to their application in various technological fields.<sup>1,2</sup> At the present time, a lot of attention is being paid to methods for the preparation of ceramic materials based on carbides, nitrides, and carbonitrides.<sup>3,4</sup> Carbonitrides are also of interest due to their usage in high-performance lithium-ion batteries for portable electronic devices. The negative electrode is made of carbon materials in all commercially available batteries. The search for new anode materials continues. Carbon-enriched  $\text{SiCN}$ ,  $\text{BCN}$ ,  $\text{Si}(\text{B})\text{CN}^{5-8}$  films are being studied for this purpose. These materials are composites of carbonitride and carbon in the form of graphite clusters or graphene sheets.

Materials with a high carbon content can be obtained from the gas phase during the decomposition of organosilicon compounds (OSC). In order to obtain silicon carbonitride by chemical vapor deposition (CVD), volatile, low-toxic, non-flammable precursor compounds are preferred.<sup>1</sup> In recent years, the synthesis of OSC, which simultaneously include all three components of silicon carbonitride, has attracted a great deal of interest.<sup>9</sup> It was found that the properties of  $\text{SiC}_x\text{N}_y$  films depend not only on the chemical composition of these compounds, but also on their structure.<sup>10–12</sup> The nature of the temperature

dependence of vapor pressure of OSC, their thermal stability at evaporation temperature, as well as a number of other properties make them suitable for use as precursors in the preparation of silicon carbonitride by CVD.

In this work we model the CVD processes of  $\text{SiC}$  and  $\text{SiC}_x\text{N}_y$  films in a flow reactor using bis(trimethylsilyl)ethylamine ( $\text{EtN}(\text{SiMe}_3)_2$ ), bis(trimethylsilyl)phenylamine ( $\text{PhN}(\text{SiMe}_3)_2$ ), and trimethylphenylsilane ( $\text{PhSiMe}_3$ )<sup>13,14</sup> in a mixture with an inert carrier gas or a chemically active gas. The starting gas mixture was introduced into the reactor, the film was deposited as a result of chemical reactions in the gas phase and on the surface of the scaffold, and the unreacted gas and gas products were removed from the reactor. The variable parameters of the process were the film deposition temperature (the substrate temperature) ( $T$ ); the carrier gas/OSC partial pressure ratio ( $q$ ) in the gas mixture introduced into the reactor; the total pressure in the reactor ( $P$ ). The calculations were carried out under the following conditions:  $T = 500\text{--}1200$  K,  $q = 0\text{--}10$ ,  $P = 0.01$ , and 10 Torr. The behavior of systems in which additional gases were: a) He, an inert component of the introduced gas mixture; b)  $\text{NH}_3$ , an active gaseous reagent used to control the nitrogen concentration in  $\text{SiC}_x\text{N}_y$  films; c)  $\text{N}_2$ , an inert component under normal conditions. It should be noted that in systems in which the gas phase introduced into the reactor was activated using high-frequency (HF) or laser radiation with the formation of a cold (for HF excitation) or hot (for laser excitation) plasma, it is, in principle, possible to activate  $\text{N}_2$  molecules, *i.e.*, promote the formation of free radicals, which will be involved in chemical reactions of

formation of  $\text{SiC}_x\text{N}_y$ . The study of the dependence of the CVD process on the change in the concentration of each single element is of particular interest.

### Experimental

Thermodynamic modeling is used for the study of gas phase processes, for example, for determining the partial pressures of molecular forms in complex gas environments.<sup>15</sup> In the present work, it was used to calculate the compositions of the gas and condensed phases during thermal decomposition of OSC in a mixture with helium or ammonia. The methodology of calculating the equilibrium is described in the work.<sup>1</sup> The following assumptions were used for the calculations.

1. The CVD process proceeds in a quasi-equilibrium regime, the composition of the system in the deposition zone is equal to the elemental composition of the input gas mixture. The gas phase in the deposition zone is in thermodynamic equilibrium with the condensed phases which form the film.

2. The gas existing in the equilibrium with the film is an ideal mixture of molecular forms (species).

3. The film is considered as a mixture of stoichiometric phases. In reality, silicon carbonitride films are amorphous phases of variable composition, sometimes containing nanocrystals of graphite,  $\text{Si}_3\text{N}_4$  and/or SiC. Therefore, we can expect that the deposition region of the amorphous film will coincide with the calculated region of co-deposition of these phases, and the average composition of a mixture of these phases and the film should be the same. We did not include amorphous silicon carbonitride in the list of phases under consideration because there is no information on its thermodynamic properties to be found in literature.

The conditions of phase equilibria were calculated using the standard data bank software "Properties of Electronics Materials" of the A. V. Nikolaev Institute of Inorganic Chemistry, Siberian Branch of the Russian Academy of Sciences,<sup>16</sup> based on the thermodynamic characteristics recommended by the reference publication.<sup>17</sup> In the calculations, the Gibbs energy of a system with a given number of elements was minimized for specified  $T$  and  $P$  values. The calculations determined the molar fractions of each of the condensed phases and each species. These data were used to plot chemical vapor deposition diagrams reflecting the deposition regions of various phases and phase complexes, depending on the composition of the gas entering the reactor and the temperature for a specified total pressure. Previously, using this approach, we modeled deposition in the Ge—C—H<sup>18</sup> and B—C—N—H<sup>19</sup> systems, as well as in the Si—C—N—H system with other precursors.<sup>1</sup>

The gas mixture introduced into the reactor consisted of volatile OSC and an additional gas taken in specified ratios. The calculations allowed for the formation of 84 molecular forms of the gas phase and six condensed phases: C (graphite), C (diamond), Si,  $\text{Si}_3\text{N}_4$ , and SiC (hexagonal and cubic structures).

## Results and Discussion

### 1. Calculation of CVD diagrams and composition of films for the $\text{EtN}(\text{SiMe}_3)_2$ —He and $\text{PhN}(\text{SiMe}_3)_2$ —He systems

The CVD diagrams, which were plotted based on calculations for two values of total pressure ( $P = 0.01$  and

10 Torr), contained regions corresponding to the deposition of a mixture of crystalline phases, namely,  $\text{Si}_3\text{N}_4 + \text{SiC} + \text{C}$  (graphite) and  $\text{SiC} + \text{C}$ , depending on the values of  $T$  and  $q$  ( $q = p_{\text{He}}/p_{\text{OSC}}$ ). It was found that the boundary  $\text{SiC} + \text{C} + \text{Si}_3\text{N}_4 \parallel \text{SiC} + \text{C}$  coincided in the diagrams for the  $\text{EtN}(\text{SiMe}_3)_2$ —He and  $\text{PhN}(\text{SiMe}_3)_2$ —He systems. Thus, it depended only on the Si : N ratio in the starting OSC and the total pressure in the system. The results of the calculation are shown in Fig. 1.

The calculation of the dependence of the average composition of the resulting mixture of phases on the deposition conditions revealed the following trends. This composition remained practically constant within the region of existence of the  $\text{SiC} + \text{C}$  phase complex and corresponded to a silicon content (in molar fractions) equal to 0.20 and 0.14 for the  $\text{EtN}(\text{SiMe}_3)_2$ —He and the  $\text{PhN}(\text{SiMe}_3)_2$ —He system, respectively. The obtained results demonstrated that the Si : C ratio in the phase mixture in both cases was lower than in the starting OSC (Si : C = 1 : 4 and 1 : 6 for  $\text{EtN}(\text{SiMe}_3)_2$  and  $\text{PhN}(\text{SiMe}_3)_2$ , respectively). Within the major part of the region of existence of the  $\text{Si}_3\text{N}_4 + \text{SiC} + \text{C}$  phase complex for the  $\text{EtN}(\text{SiMe}_3)_2$ —He system, the content of nitrogen and silicon was 0.09 and 0.18, respectively. However, the nitrogen content decreased to zero near the boundary  $\text{SiC} + \text{C} + \text{Si}_3\text{N}_4 \parallel \text{SiC} + \text{C}$ , as expected. The change in the total pressure in the systems from 0.01 to 10 Torr had little effect on the phase complex composition. As an example, Fig. 2 shows the dependence of the content of nitrogen and silicon in the complex at  $q = 3$  and  $P = 10$  Torr on temperature.

The trends of the change in content of these elements in the same complex obtained for the  $\text{PhN}(\text{SiMe}_3)_2$ —He system were similar. The content of nitrogen and silicon was 0.07 and 0.13, respectively.

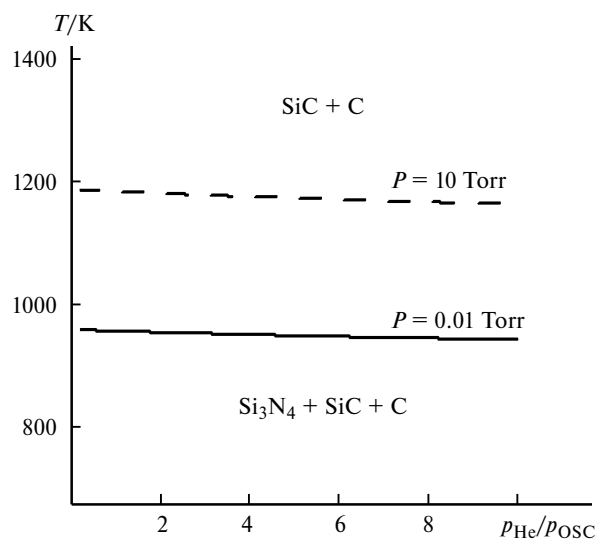


Fig. 1. CVD diagrams for the  $\text{EtN}(\text{SiMe}_3)_2$ —He and  $\text{PhN}(\text{SiMe}_3)_2$ —He systems calculated for two total pressures in the reactor.

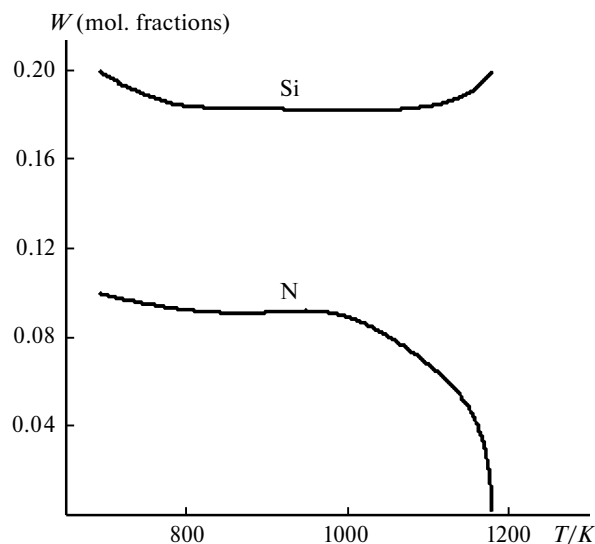


Fig. 2. Content of nitrogen and silicon ( $W$ ) calculated for the  $\text{EtN}(\text{SiMe}_3)_2\text{--He}$  system in the  $\text{SiC} + \text{C} + \text{Si}_3\text{N}_4$  phase complex at  $q = 3$  and  $P = 10$  Torr.

## 2. Calculation of CVD diagrams and composition of films for the $\text{EtN}(\text{SiMe}_3)_2\text{--NH}_3$ , $\text{PhN}(\text{SiMe}_3)_2\text{--NH}_3$ , and $\text{PhSiMe}_3\text{--NH}_3$ systems

**2.1. The  $\text{EtN}(\text{SiMe}_3)_2\text{--NH}_3$  and  $\text{PhN}(\text{SiMe}_3)_2\text{--NH}_3$  systems.** The CVD diagrams calculated for these systems are shown in Fig. 3. We note that the position of the boundaries in the diagrams for the  $\text{EtN}(\text{SiMe}_3)_2\text{--NH}_3$  and  $\text{PhN}(\text{SiMe}_3)_2\text{--NH}_3$  systems coincide. The composition of the film in the region of existence of the  $\text{SiC} + \text{C}$  complex in the investigated range of  $T$  and  $q$  was constant and could be described by the ratio  $\text{Si} : \text{C} = 1 : 6$  and  $1 : 4$  for  $\text{PhN}(\text{SiMe}_3)_2$  and for  $\text{EtN}(\text{SiMe}_3)_2$ , respectively, corresponding to the  $\text{Si} : \text{C}$  ratio in OSC.

Assuming that the obtained film was formed from graphite and silicon carbide phases, the ratio of molar amounts of  $\text{SiC} : \text{C}$  was  $1 : 5$  and  $1 : 3$  for  $\text{PhN}(\text{SiMe}_3)_2$  and  $\text{EtN}(\text{SiMe}_3)_2$ , respectively, *i.e.*, within the framework of this model, both films must be a graphite coating with inclusions of  $\text{SiC}$ .

A similar situation was observed in the region of  $\text{C} + \text{Si}_3\text{N}_4$ . The elemental composition of the film in this region can be described by the ratio  $\text{Si} : \text{N} : \text{C} = 3 : 4 : 18$  for  $\text{PhN}(\text{SiMe}_3)_2$  and  $\text{Si} : \text{N} : \text{C} = 3 : 4 : 12$  for  $\text{EtN}(\text{SiMe}_3)_2$ . Within the crystalline model of the film, the phase ratio  $\text{C} : \text{Si}_3\text{N}_4$  in these films was equal to  $18 : 1$  and  $12 : 1$ , *i.e.*, the films consisted of graphite with inclusions of silicon nitride. Within the region of deposition of three phases  $\text{C} + \text{SiC} + \text{Si}_3\text{N}_4$ , the film composition was dependent on both  $T$  and  $q$ . When these parameters were varied, the film composition smoothly changed between its values at the boundaries between the two-phase regions and the three-phase region. The total pressure in the system had little effect on the film composition in the two-phase regions, but the  $\text{C} + \text{SiC} \parallel \text{C} + \text{SiC} + \text{Si}_3\text{N}_4$  and  $\text{C} + \text{SiC} + \text{Si}_3\text{N}_4 \parallel \text{C} + \text{Si}_3\text{N}_4$  boundaries shifted toward the higher temperature region when it increased.

**2.2. The  $\text{PhSiMe}_3\text{--NH}_3$  system.** The starting organosilicon compound  $\text{PhSiMe}_3$  did not contain nitrogen; this compound was introduced into the system with ammonia. The modeling results showed a qualitative similarity in the behavior of this system and the previously considered systems with nitrogen-containing OSC. The calculated CVD diagrams are shown in Fig. 4.

We note that the  $\text{C} + \text{SiC} + \text{Si}_3\text{N}_4 \parallel \text{C} + \text{SiC}$  boundary was located near the ordinate axis at a relatively high temperature and a very low value of  $p(\text{NH}_3)/p(\text{PhSiMe}_3)$ , therefore, the low-temperature region of this boundary practically coincided with the ordinate axis in Fig. 4. The elemental composition of the film was described by the

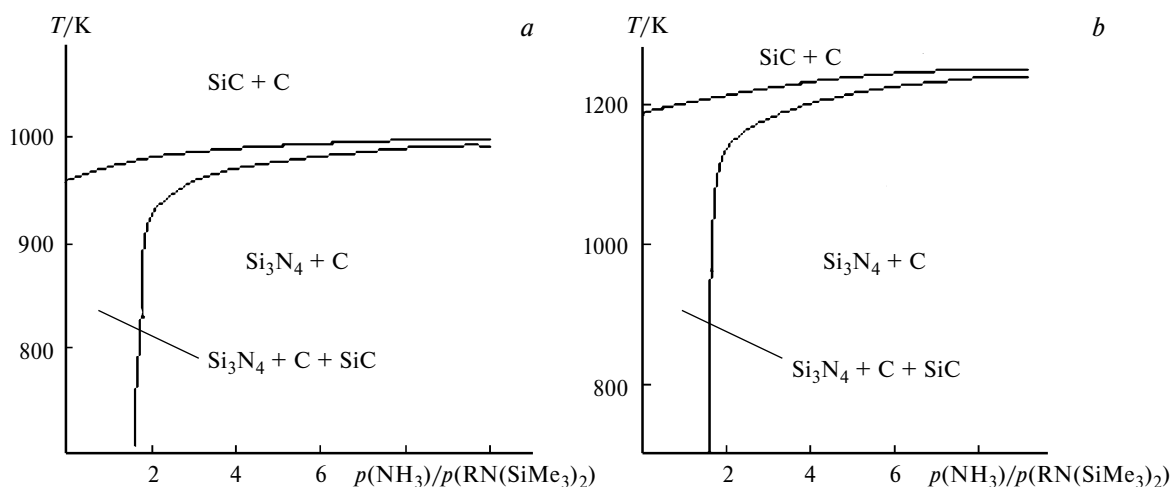


Fig. 3. CVD diagrams for the  $\text{EtN}(\text{SiMe}_3)_2\text{--NH}_3$  and  $\text{PhN}(\text{SiMe}_3)_2\text{--NH}_3$  systems calculated for two pressures in the reactor: 0.01 (a) and 10 Torr (b),  $R = \text{Ph, Et}$ .

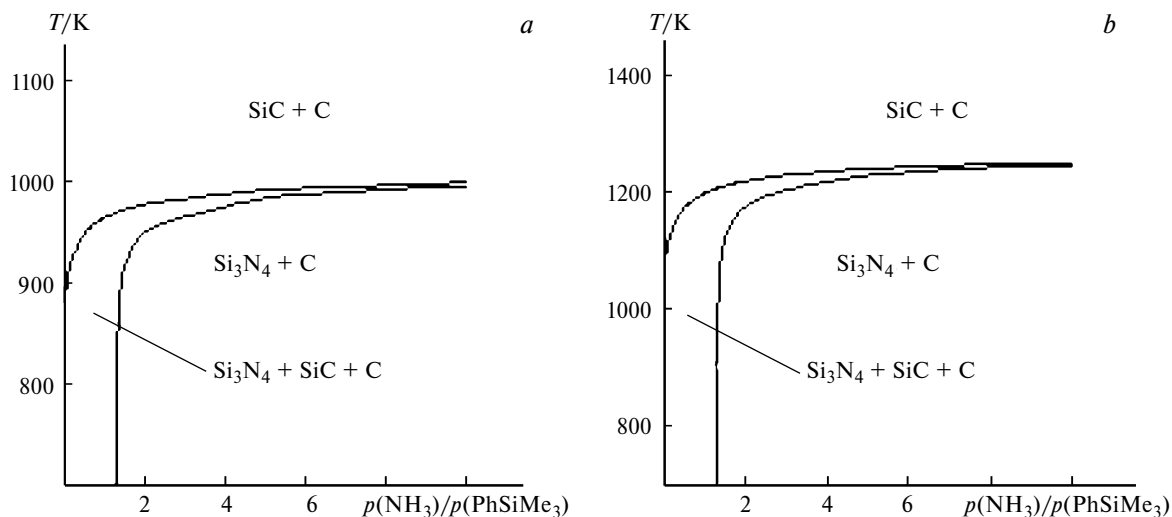


Fig. 4. CVD diagrams for the PhSiMe<sub>3</sub>—NH<sub>3</sub> system calculated for two pressures: 0.01 (a) and 10 Torr (b).

ratio Si : C = 1 : 9 at pressures equal to 0.01 and 10 Torr in the SiC + C region. Assuming that the film consisted of silicon carbide and graphite, the SiC : C phase ratio in these films was 1 : 8. In the region Si<sub>3</sub>N<sub>4</sub> + C at 0.01 Torr, the film composition was constant and corresponded to a content of C, Si, and N equal to 0.79, 0.09, and 0.12, respectively. Within the crystalline model of the film, the C : Si<sub>3</sub>N<sub>4</sub> phase ratio in these films was equal to 26 : 1. Like in the previous case, the film composition depended on both  $T$  and  $q$  in the region of deposition of the three phases C + SiC + Si<sub>3</sub>N<sub>4</sub>. When these parameters were varied, the film composition gradually changed between its values at the boundaries of the three-phase region. The same situation was observed in the high-temperature area of the Si<sub>3</sub>N<sub>4</sub> + C region in the phase diagram, but the film became slightly enriched in silicon and depleted in carbon as the temperature decreased. Reducing the temperature

and increasing the total pressure led to a decrease in the graphite content of the film in all cases.

### 3. Calculation of CVD diagrams and composition of films for the EtN(SiMe<sub>3</sub>)<sub>2</sub>—N<sub>2</sub>, PhN(SiMe<sub>3</sub>)<sub>2</sub>—N<sub>2</sub>, and PhSiMe<sub>3</sub>—N<sub>2</sub> systems

Thermodynamic analysis of these systems using nitrogen as a reagent and a carrier gas allowed us to study the effect of additives of this element only on CVD diagrams.

**3.1. The EtN(SiMe<sub>3</sub>)<sub>2</sub>—N<sub>2</sub> and PhN(SiMe<sub>3</sub>)<sub>2</sub>—N<sub>2</sub> systems.** The region boundaries in diagrams of the EtN(SiMe<sub>3</sub>)<sub>2</sub>—N<sub>2</sub> and PhN(SiMe<sub>3</sub>)<sub>2</sub>—N<sub>2</sub> systems coincided, as was the case for the diagrams described previously for these precursors. The calculation results of the CVD diagrams are shown in Fig. 5.

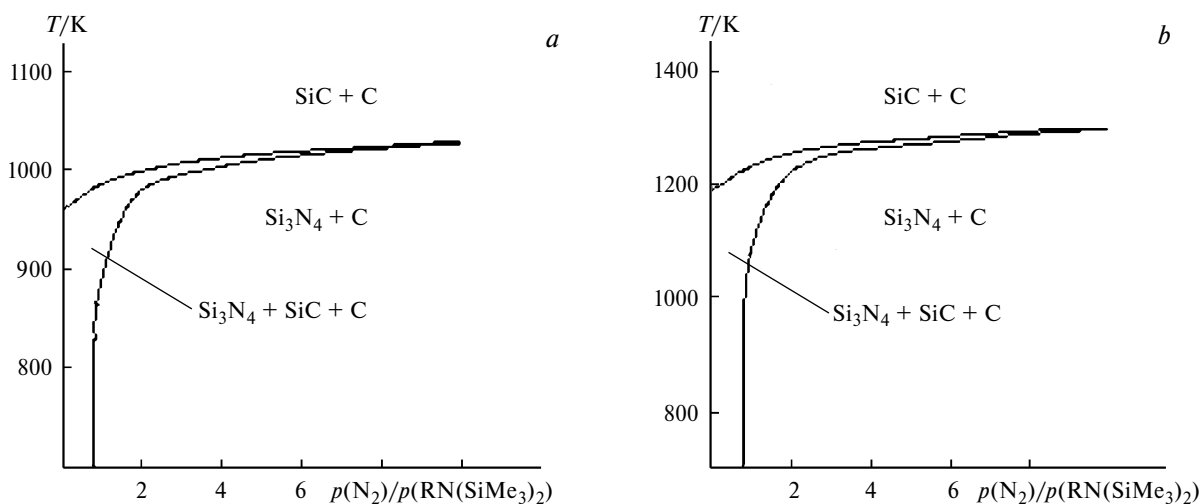
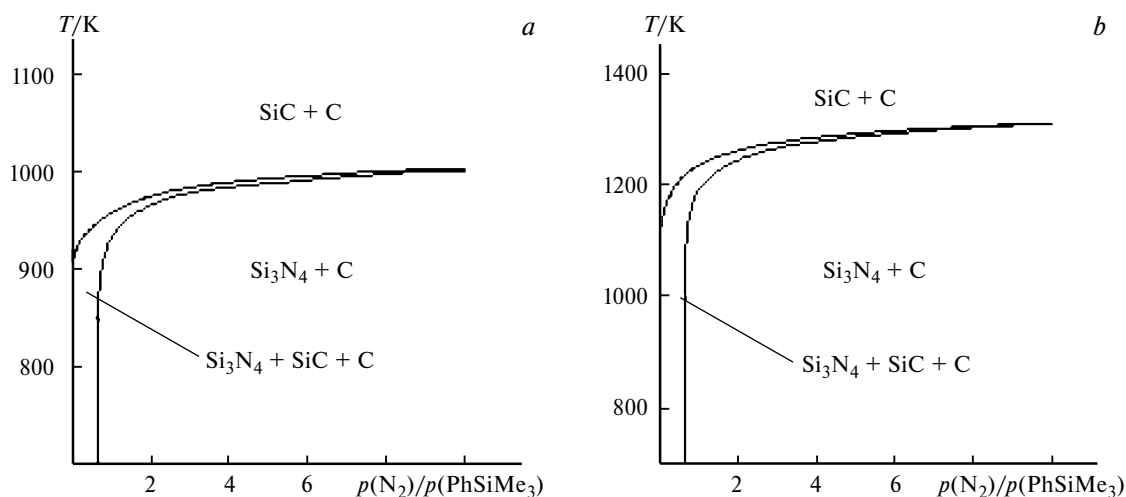


Fig. 5. CVD diagrams for the EtN(SiMe<sub>3</sub>)<sub>2</sub>—N<sub>2</sub> and PhN(SiMe<sub>3</sub>)<sub>2</sub>—N<sub>2</sub> systems calculated for two pressures: 0.01 (a) and 10 Torr (b), R = Ph, Et.



**Fig. 6.** CVD diagrams for the  $\text{PhSiMe}_3\text{--N}_2$  system calculated for two pressures: 0.01 (a) and 10 Torr (b).

A film with constant composition was deposited in the two-phase  $\text{SiC} + \text{C}$  region. When using  $\text{EtN}(\text{SiMe}_3)_2$ , the film composition was characterized by a molar ratio  $\text{Si} : \text{C} = 1 : 4$  and for  $\text{PhN}(\text{SiMe}_3)_2$  this ratio was  $1 : 6$ , *i.e.*, the same as in compounds of the starting OSC. At  $P = 0.01$  Torr, the composition of the film in the entire  $\text{Si}_3\text{N}_4 + \text{C}$  region (except a small region in the vicinity of the  $\text{SiC} + \text{Si}_3\text{N}_4 + \text{C} \parallel \text{Si}_3\text{N}_4 + \text{C}$  boundary) was characterized by the same ratios  $\text{Si} : \text{C} = 1 : 4$  and  $1 : 6$ . The molar ratio  $\text{Si}_3\text{N}_4 : \text{C}$  was  $1 : 12$  and  $1 : 18$  for  $\text{EtN}(\text{SiMe}_3)_2$  and  $\text{PhN}(\text{SiMe}_3)_2$ , respectively, *i.e.*, the film consisted mainly of carbon. At  $P = 10$  Torr, the composition of the film in the high-temperature area of the  $\text{Si}_3\text{N}_4 + \text{C}$  region is the same, and the ratio  $\text{C} : \text{Si}$  in the film decreased when the temperature decreased below 1100 K. The deposition of a three-phase  $\text{Si}_3\text{N}_4 + \text{SiC} + \text{C}$  mixture is reflected in the diagram by a narrow region on the  $q$  coordinate. At temperatures below 850 K, the composition of the film depended only on the composition of the starting OSC and its partial pressure in the gas introduced into the reactor, but was virtually independent of the deposition temperature.

**3.2. The  $\text{PhSiMe}_3 + \text{N}_2$  system.** The CVD diagram for this system (Fig. 6) contained the same phase complexes as the diagrams discussed earlier.

The specific features of the CVD diagram remained the same as those in the systems with  $\text{NH}_3$ , but the three-phase region became narrower. The composition of the film in the  $\text{SiC} + \text{C}$  region was constant, corresponding to the ratio  $\text{SiC} : \text{C} = 1 : 8$ , *i.e.*, within the framework of the crystalline model, the film consisted of graphite with inclusions of  $\text{SiC}$ . The composition of the film was constant and had a ratio  $\text{Si} : \text{C} = 1 : 9$  or  $\text{Si}_3\text{N}_4 : \text{C} = 1 : 27$  in the  $\text{Si}_3\text{N}_4 + \text{C}$  region at  $P = 0.01$  Torr, *i.e.*, the film consisted of graphite with a small number of  $\text{Si}_3\text{N}_4$  inclusions. In the intermediate region, a decrease in the partial pres-

sure of nitrogen in the starting gas mixture led to a gradual transition of nitrogen to the gas phase, with the ratio  $\text{Si} : \text{C} = 1 : 9$  remaining constant. At  $P = 10$  Torr and a temperature below 1000 K, the film became slightly enriched with silicon.

To sum up, thermodynamic modeling did not allow one to evaluate the influence of the design of the precursor molecule on the film structure and properties, since the calculation results depended only on the composition of the starting gas mixture, temperature, and total pressure in the reactor. Nevertheless, a comparison of modeling results can be useful for planning experiments to obtain carbon-enriched carbide and silicon carbonitride films. The use of compounds  $\text{EtN}(\text{SiMe}_3)_2$  and  $\text{PhN}(\text{SiMe}_3)_2$  in a mixture with helium led to the formation of two phase complexes:  $\text{SiC} + \text{C}$  (high-temperature) and  $\text{Si}_3\text{N}_4 + \text{SiC} + \text{C}$  (low-temperature). An increase of the total pressure in the system led to a shift of the boundary on the CVD diagram toward higher temperatures.

The introduction of ammonia into the starting gas mixture in all cases led to the formation of phase complexes  $\text{SiC} + \text{C} \mid \text{Si}_3\text{N}_4 + \text{SiC} + \text{C} \mid \text{Si}_3\text{N}_4 + \text{C}$ , however, it was not possible to obtain a product that did not contain elemental carbon impurities in the entire range of conditions studied. An increase in the ammonia content in the starting gas mixture led to a growth of the range of conditions suitable for obtaining products containing nitrogen.

No significant difference in the composition of the deposited products for the  $\text{EtN}(\text{SiMe}_3)_2$  and  $\text{PhN}(\text{SiMe}_3)_2$  compounds was expected. The use of trimethylphenylsilane in a mixture with ammonia made it possible to obtain the phase complex  $\text{Si}_3\text{N}_4 + \text{C}$  over a wider temperature range. It follows from the results of thermodynamic modeling that the synthesis in the presence of ammonia made it possible to obtain films of different phase composition:  $\text{SiC} + \text{C}$ ,  $\text{SiC} + \text{Si}_3\text{N}_4 + \text{C}$ ,  $\text{Si}_3\text{N}_4 + \text{C}$ . For

each case, the conditions for the co-deposition of silicon carbide and nitride phases in the temperature range below 1023 K were identified. A significant increase in  $\text{NH}_3$  content reduced the temperature interval in which co-formation of the phase complex  $\text{SiC} + \text{Si}_3\text{N}_4$  was observed. It should be noted that the application of the thermal method of gas phase activation should result in the formation of carbon clusters for all reagents in the considered temperature range. The modeling results were consistent with our experimental data on the synthesis of  $\text{SiC}_x\text{N}_y$  films enriched with carbon from trimethylphenylsilane.<sup>20</sup>

### References

1. F. A. Kuznetsov, M. G. Voronkov, V. O. Borisov, I. K. Igumenov, V. V. Kaichev, V. G. Kesler, V. V. Kirienko, V. N. Kichay, M. L. Kosinova, V. V. Kriventsev, M. S. Lebedev, A. V. Lis, N. B. Morozova, L. D. Nikulina, V. I. Rakhlin, Yu. M. Rumyantsev, T. P. Smirnova, V. S. Sulyaeva, S. V. Sysoev, A. A. Titov, N. I. Fayner, I. P. Tsyrendorzhiya, L. I. Chernyavskiy, L. V. Yakovkina, *Fundamental'nye osnovy protsessov khimicheskogo osazhdeniya plenok i struktur dlya nanoelektroniki* [Fundamentals of Processes of Chemical Deposition of Films and Structures for Nanoelectronics], Issue 37, SO RAN Publ., Novosibirsk, 2013, 176 pp. (in Russian).
2. *Silicon Carbide — Materials, Processing and Applications in Electronic Devices*, Ed. M. Mukherjee, InTech, 2011, 546 p.
3. R. M. Prasad, G. Mera, K. Morita, M. Müller, H.-J. Kleebe, A. Gurlo, C. Fasel, R. Riedel, *J. Eur. Ceram. Soc.*, 2012, **32**, 477.
4. R. Sedláč, A. Kovalčíková, V. Girman, E. Múdra, P. Rutkowski, A. Dubiel, J. Dusza, *J. Eur. Ceram. Soc.*, 2017, **37**, 4307.
5. L. M. Reinold, Y. Yamada, M. Graczyk-Zajac, H. Munakata, K. Kanamura, R. Riedel, *J. Power Sources*, 2015, **282**, 409.
6. M. Graczyk-Zajac, M. Wimmer, C. Neumann, R. Riedel, *J. Solid State Electrochem.*, 2015, **19**, 2763.
7. Sh. Bhat, P. V. W. Sasikumar, L. Molina-Luna, M. J. Graczyk-Zajac, H.-J. Kleebe, R. Riedel, *J. Carbon Res.*, 2016, **2**, 9.
8. R. Bhandavat, G. Singh, *ACS Appl. Mater. Interfaces*, 2012, **4**, 5092.
9. E. N. Ermakova, S. V. Sysoev, R. E. Nikolaev, L. D. Nikulina, A. V. Lis, I. P. Tsyrendorzhiya, V. I. Rakhlin, P. E. Plyusnin, M. L. Kosinova, *J. Therm. Anal. Calorim.*, 2016, **126**, 609.
10. N. I. Fainer, A. A. Nemkova, *High Energy Chem.*, 2015, **49**, 273.
11. E. N. Ermakova, Yu. M. Rumyantsev, V. I. Rakhlin, M. L. Kosinova, *High Energy Chem.*, 2016, **50**, 224.
12. E. Ermakova, Y. Rumyantsev, A. Shugurov, A. Panin, M. L. Kosinova, *Appl. Surf. Sci.*, 2015, **339**, 102.
13. E. N. Ermakova, S. V. Sysoev, L. D. Nikulina, I. P. Tsyrendorzhiya, V. I. Rakhlin, M. L. Kosinova, *Thermochimica Acta*, 2015, **622**, 2.
14. S. V. Sysoev, A. O. Kolontaeva, L. D. Nikulina, M. L. Kosinova, F. A. Kuznetsov, V. I. Rakhlin, A. V. Lis, M. G. Voronkov, *Glass Physics and Chemistry*, 2012, **38**, 8.
15. I. S. Aver'kov, A. V. Baykov, L. S. Yanovskiy, V. M. Volokhov, A. V. Volokhov, *Russ. Chem. Bull.*, 2016, **65**, 2004.
16. F. A. Kuznetsov, V. A. Titov, *Proc. Int. Symp. on Advanced Materials (Japan, 24—30 September, 1995)*, 1995, 16.
17. L. V. Gurvich, I. V. Veyts, V. A. Medvedev, G. A. Bergman, V. S. Yungman, G. A. Khuchkuruzov, V. S. Iorish, O. V. Dorofeeva, E. L. Osina, P. I. Tolmach, I. N. Przhival'skiy, I. I. Nazarenko, N. M. Aristova, E. A. Shenyavskaya, L. N. Gorokhov, A. L. Rogatskiy, M. E. Efimov, V. Ya. Leonidov, Yu. G. Khayt, A. G. Efimova, S. E. Tromberg, A. V. Gusarov, N. E. Khandamirova, G. N. Yurkov, L. R. Fokin, L. F. Kuratova, A. D. Gol'dshtein, *Termodinamicheskie svoystva individual'nykh veshchestv* [Thermodynamic Properties of Individual Substances], Nauka, Moscow, 1982, 623 pp. (in Russian).
18. A. N. Golubenko, M. L. Kosinova, Yu. M. Rumyantsev, F. A. Kuznetsov, *Inorgan. Mater.*, 2014, **50**, 107.
19. A. N. Golubenko, M. L. Kosinova, A. A. Titov, F. A. Kuznetsov, *Inorgan. Mater.*, 2012, **48**, 691.
20. E. Ermakova, K. Mogilnikov, Yu. Rumyantsev, V. Kichay, E. Maximovskii, O. Semenova, M. Kosinova, *Thin Solid Films*, 2015, **588**, 39.

Received October 23, 2017;  
accepted March 15, 2018